A Fast Fault Detection for Multi-Terminal VSC HVDC Transmission Lines

Jalal Sahebkar Farkhani*, S. Hassan Ashrafi Niaki, Kaiqi Ma, Claus Leth Bak, Zhe Chen
Department of energy, Aalborg University, Denmark
Emails: jsfa@energy.aau.dk, shani@energy.aau.dk, kma@energy.aau.dk, clb@energy.aau.dk, zch@energy.aau.dk
**Corresponding author*

Abstract: **The quick rise of DC short circuit current becomes a great challenge in high voltage direct current (HVDC) systems. The protection system issues of HVDC have been increasing with the presence of multi-terminal (MT) HVDC systems, in particular meshed ones. This paper proposes a fast DC fault detection scheme for MT-HVDC systems. The proposed method can detect faulted lines using only DC inductors. Moreover, this method uses the variations of inductor voltage in transmission lines (TLs) without telecommunication and it is robust against high impedance faults (HIFs). Fast fourier transform (FFT) is considered to detect the faulted line and HIF. The case study is simulated using the PSCAD/EMTDC software to evaluate the performance of the proposed method with pole-to-pole and pole-to-ground faults. The results confirm the accuracy of the proposed method.**

Keywords: **Fault Detection, DC inductors, FFT analysis, MT-HVDC**

I. INTRODUCTION

Recently, the MT-HVDC systems have been widely considered with the high penetration of renewable energy sources [1]. Although HVDC systems have many advantages such as the transmission of bulk power through long distances, underwater/underground transmissions, reducing energy loss, improving network stability, flexible and fast control ability, asynchronous interconnection of power systems, and environmental benefits [2-4]. The protection systems of HVDC are one of the most important problems due to the high fault current and fast fault propagation speed of the DC network [5].

Several research have focused on fault detection based on variations in voltage and current of HVDC systems [6-13]. In [6] presented a single-ended protection scheme based on the DC voltage across the fault current limiter (FCL) at each link end of the lines. Ref. [7] proposed a DC fault detection method based on the ratio of transient voltages of a dc inductor with main and backup protection. The main protection detects the fault without communication, while the secondary protection is based on a pilot method to detect high-impedance faults. In [8] focused on a dc fault detection and location in a meshed MT-HVDC system based on dc terminal inductances and arm inductances voltage change rate without telecommunication in a three-terminal HVDC system by parallel-series equivalent circuit. The authors in [9] proposed a protection method based on local current and voltage variations. The method used main and backup protection based on a rate of change of voltage (ROCOV) and rate of change of current (ROCOC) protection schemes, respectively. Ref. [10] presented a strategy for fault detection by a single-ended ROCOV method with high reliability and low cost. In [11] proposed a directional ROCOV value with the di/dt limiting inductors in the three-terminal HVDC. The local measurement method is used in parallel with a communication-assisted two-end ROCOV relay. In [12] presented a fast fault detection method based on the voltage gradient of the reactor. Ref. [13] proposed a fault detection based on a local measurement in the MT-HVDC systems. The main protection is based on the ROCOV method, and the ROCOC is used as the backup protection.

By expanding MT-HVDC and then creating a mesh HVDC network, the protection of future power systems becomes a great challenge. The FFT is a useful mathematical technique to analyze power systems. It is often used to transform the different signal features from the time domain to the frequency domain in signal processing-based systems [14], [15]. Ref. [16] proposed a fault detection and location technique according to gap frequency spectrum analysis in the VSC-HVDC transmission. It used the FFT technique to obtain a frequency spectrum of the fault current waveform. Ref. [17] presented a fault detection method based on the neural network, FFT, and gramian angular field (GAF) in HVDC transmission lines. The FFT is used to extract the feature data. In [18] proposed a fault detection method based on the FFT, relative principle component analysis, and support vector machine for the H-bridge multilevel inverter. The FFT is extracted the main features of voltage signals during the faults.

This paper focuses on fast fault detection in the MT-HVDC without communication systems. The method proposes fast and accurate fault detection in a four-terminal HVDC system with DC inductors. The fault detection uses variations of inductor voltage during the fault. The FFT is used to detect the faulted line and the HIF. The paper is organized as follows. Section 2 explains the theory of the proposed method. The case study and simulation results are described in Section 3, and finally, the Conclusion is presented in Section 4.

II. DESCRIPTION OF THE PROPOSED METHODOLOGY

A fast and local protection scheme is proposed to protect the DC systems in this study. The inductor voltage variations theoretical expression is given in Eq. (1):

$$V_L = L\frac{di_l}{dt} \tag{1}$$

Where L is the DC inductor value, and the di_L/dt is the change of current with time (limiting inductor values). In normal operation without the fault, the inductor voltage changes can be assumed to be zero.

$$\begin{aligned} V_L &\approx 0 \rightarrow \quad Without\ the\ Fault \\ V_L &\neq 0 \rightarrow With\ the\ Fault \end{aligned} \tag{2}$$

The proposed method is based on the local measurement as shown in Fig. (1) and a comparison of the voltage magnitudes according to Eq. (3).

$$\Delta V_L = \frac{V_{L2} - V_{L1}}{t_2 - t_1} > U_k \tag{3}$$

V_{L1} and V_{L2} are the voltage magnitudes at different measurement times of t_1 and t_2, respectively. The U_r is the reference voltage that compares with the ΔV_L. The U_r setting is considered according to the sensitivity of the systems.

$$U_r = k * U_L \tag{4}$$

where U_L is the nominal voltage of the system, and k is the coefficient that is considered 0.1 in this study. Fig. (1) shows the performance of the proposed method in MT-HVDC systems. In the fault situation, the ΔV_L is more than U_r, the faulted line will be detected by comparison of different lines that are connected to the same bus, and then both sides of each line protective relays send the trip to the circuit breaker (CB). But there is possible of maloperation of protection systems in the MT-HVDC with inductor voltage variations. Therefore, the online FFT analysis is used to detect the faulted line with the HIF. It is a standard FFT using the peak of the magnitude outputs. The simple type of CB with parallel-connected surge arresters is used to disconnect faulted lines from the network.

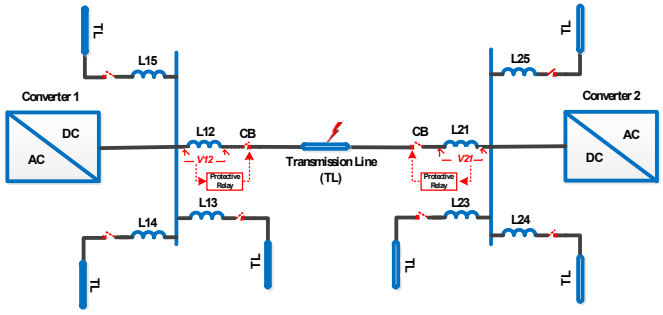

Fig. 1. Performance of proposed method in MT-HVDC

The flowchart reflects each step of the proposed method has been given in Fig. 2. First, measuring the inductor voltage (V_L) and comparing it with U_r. In a fault situation, the V_L is greater than U_r. Then, the faulted line is selected with the online FFT analysis. Of course, if the TL is one, there is no need to use the FFT analysis in order to find the faulted line.

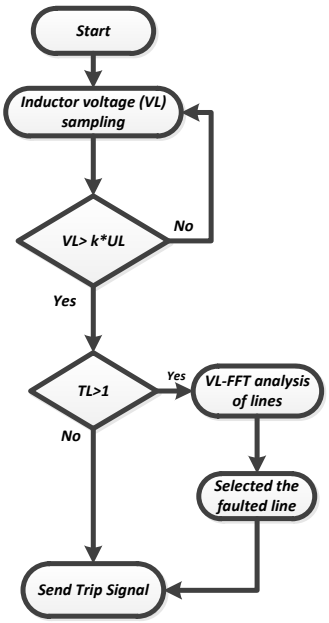

Fig. 2. Flowchart of the proposed technique

III. RESULTS

A. Case study

Fig. (3) depicts the topology of the HVDC grid with a four-terminal model in PSCAD software. The case study uses the data from the HVDC grid test system [19] for the MMC topology and cable geometry in PSCAD/EMTDC software. It consists of four converters which are converters 1, and 2 are connected to offshore AC wind farms, and converters 3, and 4 are connected to the AC grid. The dc voltage of the case study system is 640 kV. Three transmission lines of the converter1 are the candidate fault points in the case study which include pole-to-pole faults at the middle of the TL13 (Point 1), pole-to-ground fault at end of TL12 (Point 2), the pole-to-pole faults at end of TL4 (Point 3), respectively.

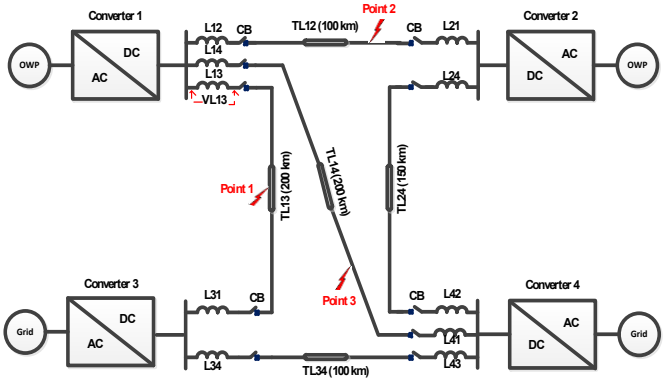

Fig. 3. Case study of the four-terminal HVDC transmission system

B. Discussion

In this section, the performance of the protection scheme is explained based on the voltage variations of dc inductors. The DC inductors can affect the transient performance, and fault current in the MT-HVDC systems [20]. Fig. (4) displays the inductors voltage variations of converter1 TLs with pole-to-pole at Point 1 and different inductors values (50 mH, 200 mH, and 300 mH). All faults are initiated at 0.51 Sec. with the setting k = 0.1. The inductor voltages which are connected to the TLs of converter 1 are changed during the fault at Point

1. Before the fault, the inductor voltage is around zero. The current fluctuations are wide during the fault due to the low impedance. The proposed fault detection can detect the fault around 2.5 mSec.

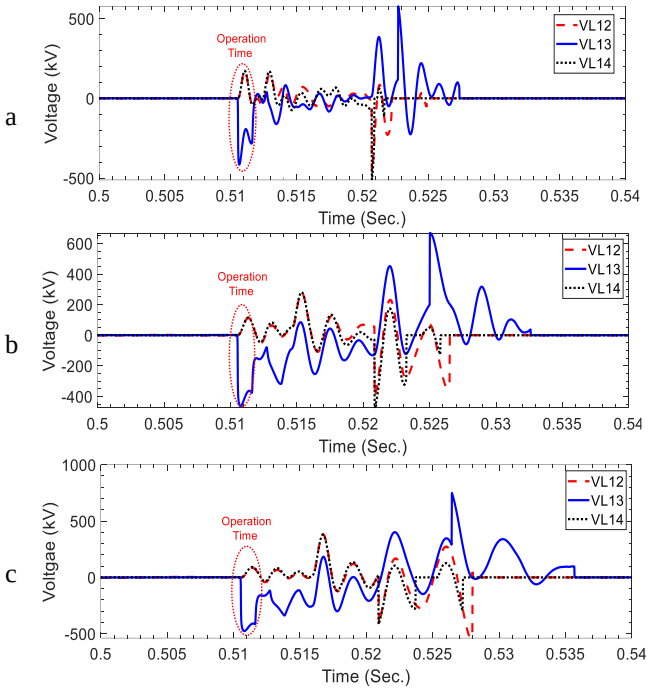

Fig. 4. Voltage variations of TLs different inductors with fault at Point1 a) inductor 50mH b) inductor 200mH c) inductor 300mH

The first peak voltage values were around 420kV, 173kV, and 172kV for L13, L14, and L12 with the inductor value of 50mH, respectively. In 200mH inductors, the initial fault voltage of L13 was 460kV and it is around 346 kV more than VL13 and VL14. The voltages L13, L14 and L12 were 480 kV, 92kV and 86kV with 300mH inductors, respectively. Increasing the inductor values causes an increase in the voltage peak of the faulted line. Therefore, it should be considered that increasing the inductor will values increase the peak of voltage and may damage the equipment. The inductor value is considered 200mH in this case study. As a result, there is possible maloperation of protection systems in the MT-HVDC TLs with inductor voltage variation.

Fig. (5) illustrates the short circuit current variations during the fault with different inductors values at Point 1. As a result, the short circuit current decreased with increasing inductor values. The maximum fault currents of inductor TL13 were around 12 kA, 8kA, and 6kA for inductors 50mH, 200mH, and 300mH, respectively. The presence of the inductor can decrease short circuit current. The maximum short circuit currents of healthy lines (inductors TL12 and TL14) were around 4.47 kA and 3.2kA for inductor 50mH, respectively. Of course, the maximum fault currents of inductors TL12 and TL14 decreased by about 2.68kA and 2kA for inductor 300mH, respectively.

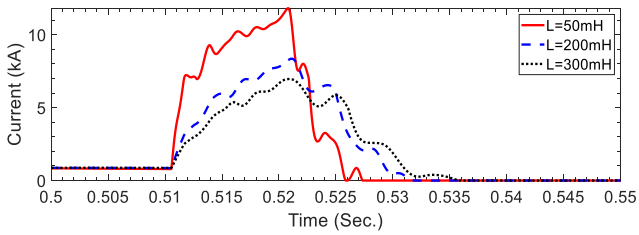

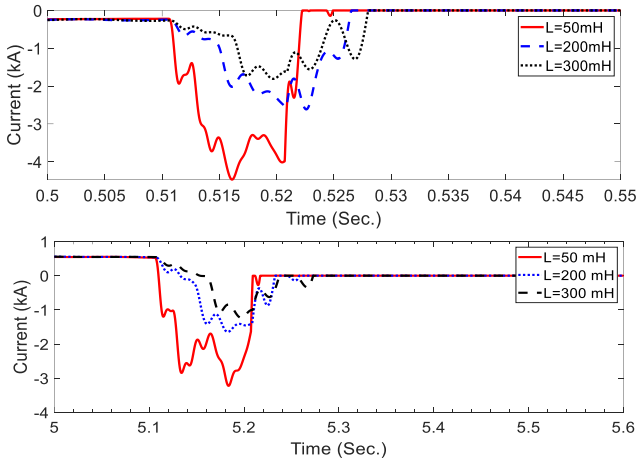

Fig. 5. The short circuit current of TLs different inductors with fault at Point 1 a) TL13 b) TL12 c) TL14

Figs. (6) and (7) display the voltage and current variations of the TLs inductors with pole-to-pole and pole-to-ground faults at Point 2 and Point 3, respectively. Fig. (6) shows the voltage and current of the TLs inductors variations during the fault at Point 2. The first peak voltage values of inductors TL12, TL13, and TL14 were around 463kV, 112kV, and 114kV, respectively. Although, the peak of VL12 was higher than other lines connected to the converter 1 busbar. The other lines' inductor voltages (VL13 and VL14) have some transients during the fault, these transients may cause the maloperation of protection systems. The maximum fault currents of inductors TL12, TL13, and TL14 were about 7.17kA, 1.86kA, and 1.46kA for fault at Point 2, respectively.

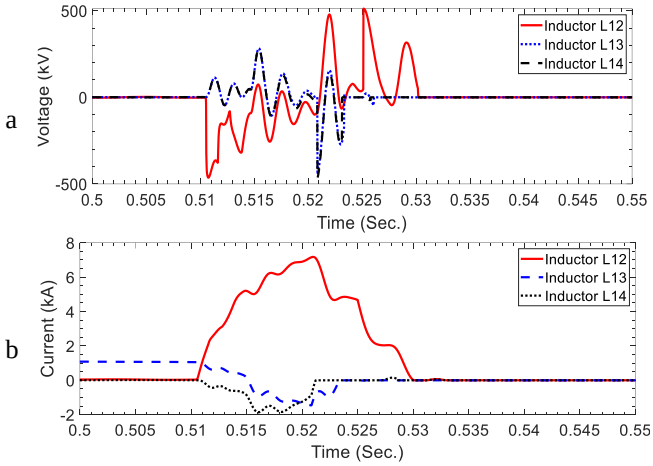

Fig. 6. The voltage and current variations of TLs inductors with fault at Point 2 a) Voltage b) Current

Fig. (7) shows the voltage and current transients of TLs inductors for the pole-to-ground fault at Point 3. As a result, the first voltage peak of VL14 is higher than other line voltages. The first peaks of voltages of VL14, VL12, and VL13 were about 363kV, 116kV, and 152kV, respectively. The maximum short circuit currents of inductors TL14, TL13, and TL12 were about 5.5kA, 0.78kA, and 1.91kA with the fault at Point 3, respectively.

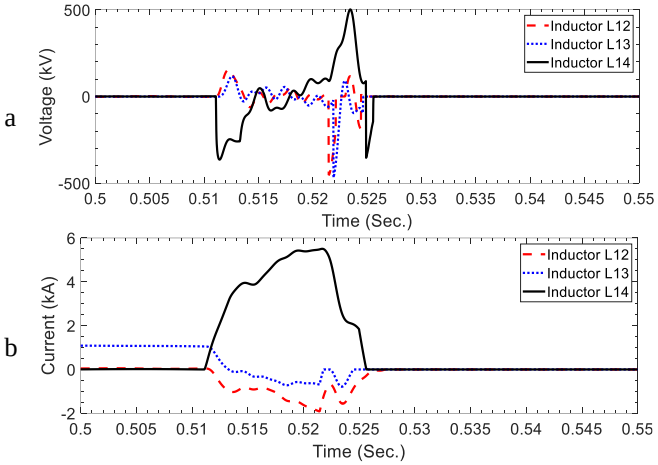

Fig. 7. The voltage and current variations of TLs inductors with fault at Point 3 a) Voltage b) Current

C. *High impedance faults*

The HIF is one of the biggest challenges of power systems protection. The HIFs lead to a decrease in the voltage and current transients during the faults. It may lead to a delay or non-tripping of protection schemes, especially current or voltage-based protection. Figs. (8) to (10) show voltage variations of inductors L13, L12, and L14 with the different HIF and faults at Points 1, 2, and 3, respectively. As a result, the voltage transient decreased by increasing the impedance of the fault. Fig. (8) displays the VL13 variations with the fault at Point 1 with different HIFs. The maximum VL13 with different HIFs were around 173kV, 83kV, 55kV, 41kV, and 30kV for 100Ω, 300Ω, 500Ω, 700Ω, and 1kΩ, respectively.

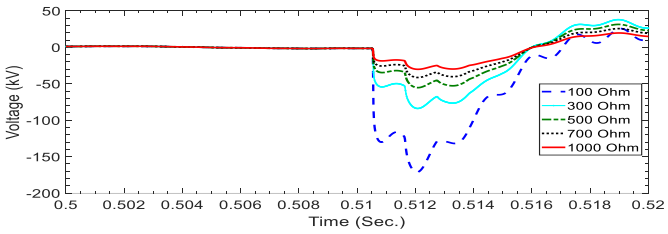

Fig. 8. VL13 variations with different HIF -faults at Point 1

Fig. (9) shows L12 inductor voltage (VL12) variations during the fault at Point 2 with different HIF. The maximum voltages of L12 were about 197kV, 114kV, 80kV, 61kV, and 45kV for 100Ω, 300Ω, 500Ω, 700Ω, and 1kΩ impedance faults, respectively.

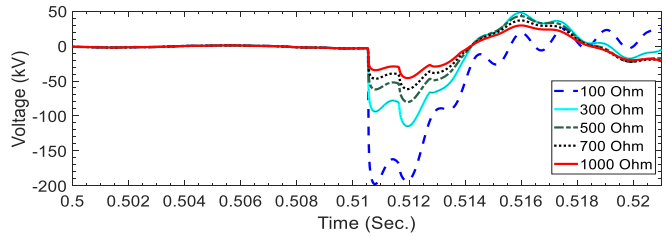

Fig. 9. VL12 variations with different HIF - Fault at Point 2

Fig. (10) displays L14 inductor voltage (VL14) variations during the fault at Point 3 with different fault impedances. The initial peak of voltage was around 100kV with the impedance fault 100Ω, while it was about 14kV during the fault with 1kΩ impedance. Therefore, it may cause maloperation of the protection system.

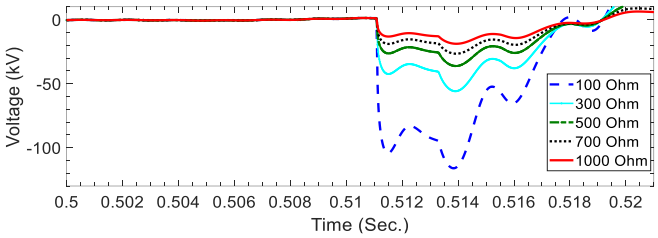

Fig. 10. VL14 variations with the different HIF- Fault at Point 3

D. *Solution*

MT-HVDC protection systems based on the inductor transients may possibly have maloperation, especially with the presence of the HIFs. Therefore, the online FFT analysis is used to detect the faulted line with the HIF. The FFT is able to transform signals from the time domain to the frequency domain in order to further analysis. Figs. (11) to (13) show transients of the inductor's voltage of the converter1 TLs (L13, L12, and L14) with the different HIF at Points 1, 2, and 3. As can be seen from the figures, the faulted line will be detected according to the initial amplitude and peak time of inductor voltage via FFT analysis. The proposed method can detect the faulted line with the HIFs as shown in the figures. Fig. (11) demonstrates the voltage variations of converter 1 TLs with fault at Point 1 and with the presence of HIFs. The initial peak of voltages with FFT analysis were around 47.8kV, 3.7kV, and 5.04kV for VL13, VL12, and VL14 with 100Ω impedance fault, respectively. In the 1kΩ impedance fault, initial maximum voltages of VL13, VL12, and VL14 were about 11.42kV, 0.35kV, and 1.34kV, respectively.

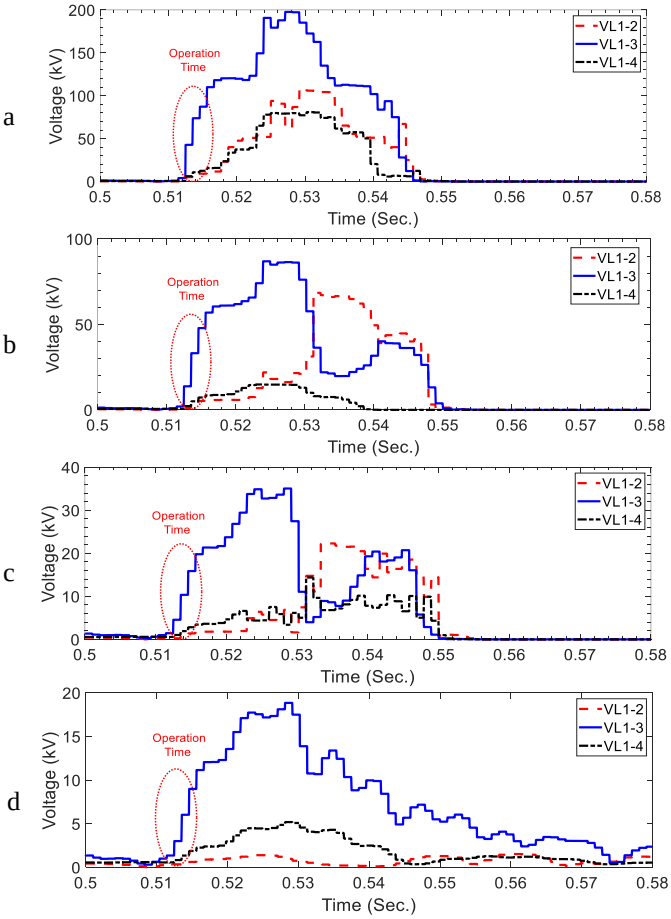

Fig. 11. The FFT voltage analysis of inductors TLs with the fault at Point 1 and HIFs a) without HIF b) 100 Ω c) 500 Ω d)1000 Ω

Fig. (12) displays the FFT analysis with the different HIFs and faults at Point 2. Although increasing the impedance of fault leads to a decrease in the amplitude of the voltage. The proposed method can detect the fault with the HIFs. The initial maximum voltages were around 52.19kV, 4.7kV, and 6.3kV for VL12, VL13, and VL14 with 100 Ω impedance faults, respectively. In the 1000 Ω impedance fault, the initial maximum voltages of VL12, VL13, and VL14 were about 11.86kV, 2.2kV, and 1.32kV, respectively.

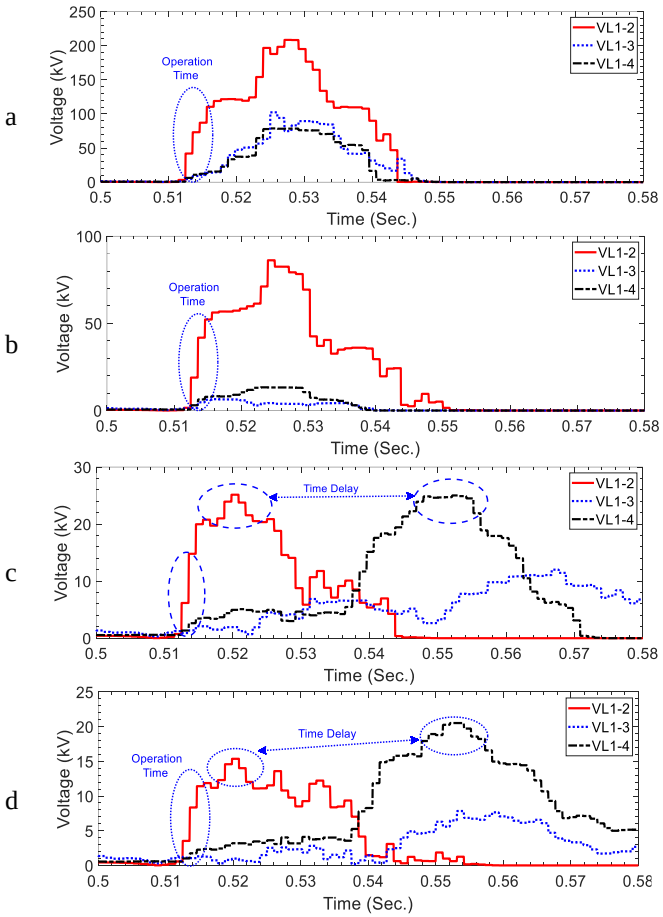

Fig. 12. The FFT voltage analysis of inductors TLs with the fault at Point 2 and HIFs a) without HIF b) 100 Ω c) 500 Ω d)1000 Ω

Fig. (13) shows the FFT analysis with the different HIFs and pole-to-ground fault at Point 3. As a result, the proposed method can detect the faulted lines with the HIF. In 100 Ω impedance fault, the initial maximum voltages of VL14, VL13, and VL12 were about 37.24kV, 8.12kV, and 7.9kV, respectively.

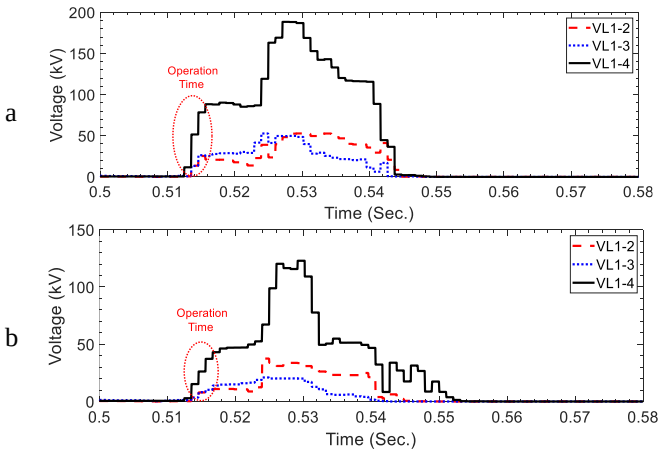

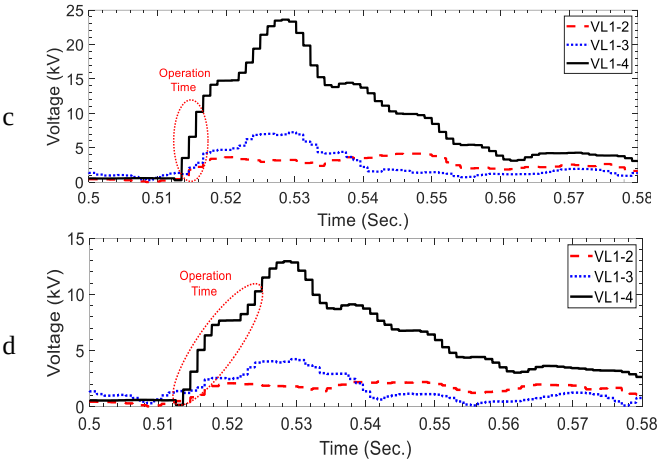

Fig. 13. The FFT voltage analysis of inductors TLs with the fault at Point 3 and HIFs a) without HIF b) with 100 Ω c) with 500 Ω d)1000 Ω

IV. CONCLUSIONS

Expanding MT-HVDC transmission lines and then creating a mesh HVDC network make the protection of future power systems a great challenge. This paper proposed a high-speed fault detection scheme for MT-HVDC systems. As a result, protection systems may maloperation in MT-HVDC networks. The proposed method only uses the inductor voltage transients of the transmission lines without telecommunication systems and is not dependent on the power flow direction. Moreover, this method is robust against fault impedance. The FFT was used to analyze the fault and detect the faulted lines with HIFs according to the initial amplitude and peak time. The presence of the inductor can reduce the short circuit current and prevent damage to the converter. The method was tested in different lines with the pole-to-pole and pole-to-ground faults and HIFs. The simulation results confirm the accuracy of the proposed method.

REFERENCES

[1] Y. Wu, S. Peng, Y. Wu, M. Rong, and F. Yang, "Technical Assessment on Self-Charging Mechanical HVDC Circuit Breaker," *IEEE Trans. Ind. Electron.*, vol. 69, no. 4, pp. 3622–3630, 2021.

[2] P. Wang, P. Liu, T. Gu, N. Jiang, and X.-P. Zhang, "Small-Signal Stability of DC Current Flow Controller Integrated Meshed Multi-Terminal HVDC System," *IEEE Trans. Power Syst.*, vol. 38, no. 1, pp. 188–203, 2022

[3] H. Wang and M. A. Redfern, "The advantages and disadvantages of using HVDC to interconnect AC networks," *45th International Universities Power Engineering Conference UPEC2010*, 2010, pp. 1–5.

[4] X. Liang and M. Abbasipour, "HVDC Transmission and Its Potential Application in Remote Communities: Current Practice and Future Trend," *IEEE Trans. Ind. Appl.*, vol. 58, no. 2, pp. 1706–1719, 2022.

[5] S. H. A. Niaki, Z. Liu, Z. Chen, B. Bak-Jensen, and S. Hu, "Protection System of Multi-Terminal MMC-based HVDC Grids: A Survey," *2022 International Conference on Power Energy Systems and Applications (ICoPESA)*, 2022, pp. 167–177.

[6] M. J. Pérez-Molina, P. Eguia, D. M. Larruskain, E. Torres, O. Abarrategi, and J. C. Sarmiento-Vintimilla, "Single-ended limiting inductor voltage-ratio-derivative protection scheme for VSC-HVDC grids," *Int. J. Electr. Power Energy Syst.*, vol. 147, p. 108903, 2023.

[7] C. Li, A. M. Gole, and C. Zhao, "A fast DC fault detection method using DC reactor voltages in HVdc grids," *IEEE Trans. Power Deliv.*, vol. 33, no. 5, pp. 2254–2264, 2018.

[8] J. Liu, N. Tai, and C. Fan, "Transient-voltage-based protection scheme for DC line faults in the multiterminal VSC-HVDC system," *IEEE Trans. Power Deliv.*, vol. 32, no. 3, pp. 1483–1494, 2016.

[9] M. J. Pérez-Molina, D. M. Larruskain, P. Eguía, and V. V. Santiago, "Local Derivative-Based Fault Detection for HVDC Grids," *IEEE Trans. Ind. Appl.*, vol. 58, no. 2, pp. 1521–1530, 2021.

[10] R. Li and L. Yao, "DC Fault Detection and Location in Meshed Multiterminal HVDC Systems Based on DC Reactor Voltage Change Rate," *IEEE Trans. POWER Deliv.*, vol. 32, no. 3, 2017, doi: 10.1109/TPWRD.2016.2590501.
[11] N. M. Haleem and A. D. Rajapakse, "Application of new directional logic to improve DC side fault discrimination for high resistance faults in HVDC grids," *J. Mod. Power Syst. Clean Energy*, vol. 5, no. 4, pp. 560–573, 2017.
[12] M. Hassan, M. J. Hossain, and R. Shah, "DC fault identification in multiterminal HVDC systems based on reactor voltage gradient," *IEEE Access*, vol. 9, pp. 115855–115867, 2021.
[13] M. J. P. Molina, D. M. L. Escobal, P. E. Lopez, and V. V. Santiago, "Fault detection based on ROCOV and ROCOC for multi-terminal HVDC systems," *2020 IEEE 20th Mediterranean Electrotechnical Conference (MELECON)*, 2020, pp. 506–511.
[14] B. N. Mohapatra and R. K. Mohapatra, "FFT and sparse FFT techniques and applications," *2017 Fourteenth International Conference on Wireless and Optical Communications Networks (WOCN)*, 2017, pp. 1–5.
[15] S. Rapuano and F. J. Harris, "An introduction to FFT and time domain windows," *IEEE Instrum. Meas. Mag.*, vol. 10, no. 6, pp. 32–44, 2007.
[16] Q. Yang, S. Le Blond, B. Cornelusse, P. Vanderbemden, and J. Li, "A novel fault detection and fault location method for VSC-HVDC links based on gap frequency spectrum analysis," *Energy Procedia*, vol. 142, pp. 2243–2249, 2017.
[17] C. Ding, Z. Wang, Q. Ding, and Z. Yuan, "Convolutional neural network based on fast Fourier transform and gramian angle field for fault identification of HVDC transmission line," *Sustain. Energy, Grids Networks*, vol. 32, p. 100888, 2022.
[18] T. Wang, J. Qi, H. Xu, Y. Wang, L. Liu, and D. Gao, "Fault diagnosis method based on FFT-RPCA-SVM for cascaded-multilevel inverter," *ISA Trans.*, vol. 60, pp. 156–163, 2016.
[19] W. Leterme, N. Ahmed, J. Beerten, L. Ängquist, D. Van Hertem, and S. Norrga, "A new HVDC grid test system for HVDC grid dynamics and protection studies in EMT-type software," *11th IET International Conference on AC and DC Power Transmission*, 2015, pp. 1–7.
[20] J. S. Farkhani, K. Ma, Z. Chen, and C. L. Bak, "Comparison of Different Types of FCLs effect on the Transient of VSC MT-HVDC System," *IEEE Canada Electrical Power and Energy Conference (EPEC)*, 2022.